MOLECULAR BEAM EPITAXY OF II-VI COMPOUND WAVEGUIDES

Donald L. Smith

Perkin-Elmer Corporation

Prepared for:

Office of Naval Research
Advanced Research Projects Agency

25 March 1974

TECHNICAL REPORT

1 July 1973 - 28 February 1974

ARPA Order No. 2327

Program Code No. 3D10

Contractor:
Perkin-Elmer Corporation

Effective Date of Contract:
1 March 1973
(received 28 June 1973)

Contract Expiration Date:
30 June 1974

Amount of Contract: $67,000.00

Contract No. N00014-73-0280

Principal Investigator:
Dr. Donald L. Smith
203-762-6916

Scientific Officer:
Director, Naval Research Laboratory

Title: Molecular Beam Epitaxy of II-VI Compound Waveguides

Sponsored by

Advanced Research Projects Agency

ARPA Order No. 2327

Unclassified

SECURITY CLASSIFICATION OF THIS PAGE (When Data Entered)

AD-778354

REPORT DOCUMENTATION PAGE

READ INSTRUCTIONS BEFORE COMPLETING FORM

1. REPORT NUMBER	2. GOVT ACCESSION NO. / 3. RECIPIENT'S CATALOG NUMBER
4. TITLE (and Subtitle): MOLECULAR BEAM EPITAXY OF II-VI COMPOUND WAVEGUIDES	5. TYPE OF REPORT & PERIOD COVERED: Technical Report 1 July '73 - 28 Feb. '74
	6. PERFORMING ORG. REPORT NUMBER: 11878
7. AUTHOR(s): Dr. Donald L. Smith	8. CONTRACT OR GRANT NUMBER(s): N00014-[redacted]-73-C-0280
9. PERFORMING ORGANIZATION NAME AND ADDRESS: The Perkin-Elmer Corporation, Optical Group Research Department, Norwalk, Conn. 06856	10. PROGRAM ELEMENT, PROJECT, TASK AREA & WORK UNIT NUMBERS
11. CONTROLLING OFFICE NAME AND ADDRESS: Advanced Research Projects Agency, Office of Naval Research	12. REPORT DATE: March 25, 1974
	13. NUMBER OF PAGES: 57
14. MONITORING AGENCY NAME & ADDRESS (if different from Controlling Office)	15. SECURITY CLASS. (of this report): Unclassified
	15a. DECLASSIFICATION/DOWNGRADING SCHEDULE

16. DISTRIBUTION STATEMENT (of this Report)

17. DISTRIBUTION STATEMENT (of the abstract entered in Block 20, if different from Report)

18. SUPPLEMENTARY NOTES

19. KEY WORDS (Continue on reverse side if necessary and identify by block number)

epitaxy; vacuum evaporation, II-VI semiconductors; optical waveguides

20. ABSTRACT (Continue on reverse side if necessary and identify by block number)

Thin films of ZnSe, ZnTe, Zn(SeTe), Cd(SeTe) and CdTe were grown on CdS, CdSe, CaF_2, and sapphire substrates by evaporation of the elements under ultra-high vacuum. Substrate chemical polishing techniques were developed. Elemental and compound evaporation and deposition rates were measured by mass spectrometer, film thickness, and quartz crystal microbalance. Compounds grew at temperatures far

DD FORM 1 JAN 73 1473 EDITION OF 1 NOV 65 IS OBSOLETE

SECURITY CLASSIFICATION OF THIS PAGE (When Data Entered)

above those at which elements alone would condense, but well below the compound decomposition temperatures. Most excess impinging group II or VI element was re-evaporated from the growing films. Films were analyzed by LEED and Auger spectroscopy. Monocrystalline films were obtained over narrow substrate temperature ranges, below which films were polycrystalline and above which deposition ceased. Monocrystalline, (111)-oriented films exhibited coarsly-faceted surfaces unsuitable for optical coupling. Polycrystalline film waveguides had high propagation losses. Growth on other planes may eliminate the faceting problem and produce low-loss waveguides.

TABLE OF CONTENTS

I. SUMMARY

This work was concerned with generating high-quality single-crystal thin films of II-VI compound semiconductors for ultimate use as electro-optically active (index-modulating) elements in integrated optical circuits. We employed the relatively unexploited film growth technique of molecular beam epitaxy, a sophisticated modification of vacuum evaporation, because of its demonstrated unique ability to generate exceptionally smooth films and multi-layer structures with precisely defined geometries and sharp interfaces, properties of particular value in integrated optics applications. We were specifically concerned with optimizing the growth parameters for generating films of zinc and cadmium selenides and tellurides and with evaluating these films by examining waveguiding properties. Films were grown on heated, single-crystal substrates under ultra-high vacuum by deposition of pure elements evaporated from liquid nitrogen-shrouded graphite Knudsen cells. Films were analyzed in situ, crystallographically by low-energy electron diffraction and chemically by Auger electron spectroscopy.

Elemental deposition rates were determined from vapor pressure data, film thickness, and quartz crystal microbalance monitoring. Discrepancies of factors of two in

these data pointed up the need for continuous process monitoring using the quartz crystal. The quartz crystal also revealed that at sufficiently high substrate temperatures most excess impinging group II or VI vapor was re-evaporated from the growing II-VI compound film, so that growth rate was determined by the impingement rate of the deficient element. A small fraction of the excess element was incorporated into the growing compound, producing intrinsic doping. This fraction varied considerably among elements and compounds. Process control using continuous quartz crystal monitoring should minimize this effect.

Chemical polishing techniques were developed for CdS (0001A) and CdSe(0001A) substrates which produce completely featureless, undistorted single-crystal surfaces ideal for epitaxial growth. This work has been submitted for publication. On these substrates we achieved single-crystal growth of ZnSe, ZnTe, Cd(SeTe) and CdTe. However, the single-crystal films had coarse-textured surfaces, presumably due to faceting to other crystallographic planes. For all of the compounds, single-crystal growth occurred over a narrow temperature range just below the compound decomposition temperature. At lower temperatures, films simultaneously became polycrystalline and mirror-smooth. 6328Å light was coupled into several of the smooth ZnSe and ZnTe films, and film thicknesses and refractive indices calculated

from coupling angles agreed closely with known values. Propagation losses were relatively high, however, presumably due to scattering from grain boundaries, and therefore infrared coupling was not attempted. Single-crystal films could not be coupled into due to surface roughness.

Effort was concentrated on (0001)-oriented growth because of symmetry between cubic and hexagonal crystal systems along that plane and because of superior electro-optic properties. Further effort should explore growth on other planes in an attempt to simultaneously achieve smooth-surfaced and monocrystalline films. It is likely that such films will be obtainable once the preferred growth plane is discovered.

II. EXPERIMENTAL SYSTEM

II-VI compound films produced under this contract were grown by molecular beam epitaxy, a highly-controlled form of classical vacuum evaporation. Figure 1 is a schematic of our two-chamber 10^{-10} Torr vacuum system. The growth chamber is to the left of the isolation valve, the preparation and analysis chamber is to the right. Films are analyzed <u>in situ</u> for crystallography by low-energy electron diffraction (LEED) and for elemental surface composition by Auger spectroscopy. The gas valves and ion gun are for substrate cleaning. Source materials evaporate from six liquid nitrogen-shrouded graphite Knudsen cells, held isothermal to $\pm 1^{\circ}C$. The mass spectrometer monitors evaporant flux and detects contamination. The shutter permits instantaneous starting and stopping of growth. The five-position substrate holder minimizes downtime. Each substrate has a thermocouple probe buried in a 0.3mm diameter by 3mm deep hole in its edge for precise temperature control during growth. Specifications of source materials used in this work are listed in Table I.

A typical run proceeded as follows. Substrates were installed with the growth chamber under vacuum, and the preparation chamber was baked to achieve 10^{-10}Torr. Sub-

strates were heat-cleaned and examined by LEED. Knudsen cells were brought to operating temperature, and effusion was checked with the mass spectrometer. Substrates were advanced into the growth chamber and brought to growth temperature with the shutter closed. The shutter was opened for the desired growth time, then closed, and the grown film was retracted into the analysis chamber for analysis by LEED and Auger spectroscopy. Knudsen cell effusion was re-checked with the mass spectrometer before shutdown. Films were removed from the chamber for visual examination, for thickness measurement by Michelson interferometry and for waveguiding experiments.

III. RESULTS

A. Substrate Preparation

Considerable effort was expended on developing chemical polishing techniques for CdS and CdSe substrates, since the quality of grown films is directly dependent on substrate quality. Single crystal film growth requires single crystal substrates with undistorted surfaces, and low scatter-loss waveguides require that these surfaces be mirror-smooth as well. The simultaneous satisfaction of these two requirements requires particular care.

The procedure reported for CdSe in the January Quarterly Report was submitted for publication to the Journal of the Electrochemical Society, and the manuscript is included here as the Appendix. In addition, a procedure was developed for CdSe which gives (0001A) surfaces completely featureless under 400X Nomarski microscope examination and (0001B) surfaces showing barely detectable irregularity. A and B (Cd and Se) faces were distinguished by the etching procedure of ref. 14. The LEED pattern obtained after only a 1-minute vacuum firing at 400°C shows the bright, sharp beams and low background characteristic of undistorted single-crystal surfaces (Fig. 2). The polishing solution consisted of 5 parts household bleach (dilute NaOCl), 5 parts

water, and 1 part precipitated silica, by volume. Substrates were loaded to 370 grams/cm^2 on a Geoscience Corp. Politex Supreme polishing pad moving at 200 rpm.

The CdSe procedure evolved much more quickly than did the CdS. While this may have been fortuitous, we feel it indicates the achievement of a certain expertise in this area which will prove valuable in fulfilling future substrate needs.

B. Deposition Monitoring

Monitoring and control of element evaporation continues to be one of the more demanding aspects of molecular beam epitaxy. Figure 4 shows the impingement rates of the elements Zn, Cd, Se, and Te at the substrate as functions of Knudsen cell temperature. The solid curves were calculated from available vapor pressure data[1] and from the Knudsen effusion equation[2]:

$$W = \frac{8.8 \times 10^{21} d^2 P}{R^2 \sqrt{MT}} \qquad (1)$$

W = vapor flux at orifice normal, molecules/ cm^2 sec

d = orifice diameter, cm

P = vapor pressure, Torr

R = distance from orifice, cm

M = vapor molecular weight, amu

T = cell temperature, ^oK

Relative abundances of Se vapor species are given by Berkowitz and Chupka.[3] Flux is seen to be quite strongly temperature-dependent, typically several percent per degree. Zn and Te_2 calibrations made by measuring deposition on 77^oK substrates (reported in January) are seen to be a factor of two lower than the vapor pressure data. This discrepancy reflects the combined errors in measurement of P, T, d, and R. Difficulty in correlating thickness of grown II-VI compound films with this data to better than a factor of two has suggested that drift in these calibrations is also taking place. A continuous monitoring method is clearly needed. The mass spectrometer has been used here and elsewhere[4,5], but is subject to sensitivity drift and background signal from re-evaporating species and is an indirect measurement, in that it is not actually monitoring the deposition.

The frequency shift of a quartz oscillator due to loading with an evaporant has long been used to monitor vacuum-evaporated film growth, but has not been applied to epitaxial growth because of the high substrate temperatures involved. Since growth kinetics are critically dependent on substrate temperature, the monitor crystal must be held at the actual film growth temperature. Under these conditions the quartz is very frequency-unstable, and in addition the conventional Ag and Au electrodes react with the impinging molecules. We have developed, using internal funds, a special isothermal mount and sputtered Nb electrodes which have allowed us to make growth rate measurements at temperatures up to 400°C for all of the II-VI compounds to an accuracy of about .01 microns/hr. (1/100 monolayer/sec). At fixed quartz crystal temperatures of 200° for CdSe and 300° for the other binaries, growth rate was measured as a function of the group II element cell temperature at constant group VI element cell temperature, and vice versa. These data are plotted in Fig. 5a-h. Figure 5d, for example, shows the effect on ZnTe growth rate of Te cell temperature when Zn cell temperature is held constant. As cell temperature, and therefore Te_2 flux at the substrate increases, so does growth rate. The solid line has been drawn with the slope of the elemental flux data of Fig. 4, and growth rate data are seen to have the same slope,

providing a good check on the accuracy of the quartz monitoring technique. In this region of increasing growth rate, growth rate is governed by Te_2 flux, and excess Zn re-evaporates from the growing ZnTe due to the elevated substrate temperature (300°C). When Te_2 rate becomes excess, growth is Zn-limited, and most excess Te_2 re-evaporates, but the slight slope suggests that some is being incorporated into the film, causing intrinsic doping. This slope, and hence the extent of intrinsic doping, is seen to vary considerably from compound to compound and element to element, being steepest for excess Zn in ZnSe (Fig. 5a) and levelest for excess Se in CdSe (Figure 5f). The effects of non-stoichiometric growth conditions may thus be predicted. Auger spectroscopy data reported in October for ZnTe films grown under excess-Zn and excess-Te conditions showed film composition to be constant to ±10%. The quartz crystal can sense the small deviations from stoichiometry taking place within this range, and in addition has the potential for continuous growth monitoring. The highest-quality material should of course be obtained at the knee (circled point) and we hope to eventually feedback-control the process to remain on that point.

If it is assumed that, for growth at the knee of Figs. 5a-h, all impinging molecules are incorporated into the film, then elemental impingement rates may be calculated from compound growth rates measured by the quartz crystal,

using the data in Table II. These calculated rates have been plotted in Figures 4a-d, and are seen to be in close agreement with the vapor pressure slopes and within a factor of two of the vapor pressure and elemental deposition calibrations, except in the case of Cd, whose vapor pressure is apparently nearly an order of magnitude lower than quoted in reference 1. If instead, only 1/10 of impinging Cd were being incorporated into the film, the knee in Fig. 5f would be much less sharp. It is particularly interesting to note that all of the Se is being incorporated into the films (Fig. 4c), because polyatomic species are often found to have very low sticking coefficients due to steric hinderance.

C. Compound Evaporation

The October Quarterly Report contained a study of ZnTe evaporation. As ZnTe was evaporated from the Knudsen cell at various temperatures, the pressures of the vapor species (Zn and Te_2) were measured by the mass spectrometer after the mass spectrometer had been calibrated for these species by evaporation of the pure elements. The equilibrium constant for the reaction

$$(ZnTe)_s \rightleftarrows (Zn)_g + \tfrac{1}{2}(Te_2)_g \qquad (2)$$

is given by

$$K_p = P_{Zn}^2 P_{Te_2} \quad (Torr^3) \qquad (3)$$

and for thermodynamic consistency this constant must obey the relationship[6]

$$\log K_p \sim 1/T \qquad (4)$$

Figure 6 shows that K_p calculated from our P data does obey this relationship and that in addition it agrees exactly with and extends the data of Goldfinger and Jeunehomme[7], the discrepancy present in the Quarterly Report having been a plotting error. This result substantiates the pressure and temperature measurement techniques of both ref. 7 and ourselves.

The re-evaporation rate from a growing II-VI compound surface may be calculated from K_p as follows. From the kinetic theory of gases, evaporation rate from a surface is related to the equilibrium vapor pressure over that surface by[1]

$$J = \frac{3.5 \times 10^{22} P}{\sqrt{MT}} \qquad (5)$$

J = molecules/cm^{2}sec.

Since group II and VI elements are much more volatile than their compounds, evaporation is congruent, so that

$$J_{Zn} = 2J_{Te_2} \tag{6}$$

Combining equations 3, 5 and 6,

$$J_{ZnTe} = J_{Zn} = \frac{4.42 \times 10^{22} K_p^{1/3}}{T^{1/2} M_{Zn}^{1/3} M_{Te_2}^{1/6}} \tag{7}$$

From equation 7, the data in Table II and extrapolations of known K_p[7], compound re-evaporation rates were calculated as functions of temperature and are plotted in Fig. 7. These rates determine the absolute upper limits to II-VI compound growth temperatures, quantities of prime importance in optimizing growth conditions.

D. Film Growth

Under this contract, films of ZnSe, Zn(SeTe), ZnTe, CdSe, Cd(SeTe) and CdTe have been grown on CaF_2, sapphire, CdS, and CdSe single-crystal substrates. The more significant of these runs are listed in Table III. Films grown on CaF_2 could not be analyzed by LEED due to surface charging, although some revealed their degree of crystallinity by cracking into mosaic patterns from thermal strain, as reported in October. Films on which neither crystallinity nor waveguiding measurements could be made, or which were obviously contaminated, or for which there was a processing failure,

are not tabulated. Sticking coefficient is defined here as the ratio of actual growth rate to elemental impingement rate. Actual growth rates were calculated from interferometric film thickness measurements ($\pm$.03 microns) and from growth times. Impingement rates are accurate to a factor of two, as discussed in section B. Waveguiding measurements are discussed in section E.

The effects of growth rate and temperature on film appearance and crystallography are seen from Table III to be similar for the various compounds grown. At the lower substrate temperatures, all films are mirror-smooth and polycrystalline. At higher temperatures, monocrystalline films were obtained for all compounds except Zn(SeTe) over about a 50° range of temperature, above which the sticking coefficient drops rapidly towards zero. The temperature at which the sticking coefficient drops off increases somewhat with growth rate. Since the sticking coefficient always drops off before film re-evaporation rate (as determined from Fig. 7) becomes significant, growth temperature is apparently being limited instead by the re-evaporation of the impinging elements before reaction to the compound. The single exception to this was ZnTe film No. 17, whose growth was initiated at 350°C and completed at 450°C, which

corresponds to a re-evaporation rate of 0.5 microns/hr. The presence of an initial ZnTe deposit seems to have decreased considerably the re-evaporation rates of impinging Zn and Te_2, allowing growth at the higher temperature.

When films changed from polycrystalline to monocrystalline upon increasing substrate temperature, they also became progressively rougher in appearance, except in cases of films so thin that such roughness was not yet visible (Nos. 3, 12, 14 and 23). This suggests faceting, or growth of surface pyramids to expose crystallographic planes other than the growth plane. In the case of film No. 1, "maverick" LEED beams produced by surface planes inclined to the substrate provided direct evidence of faceting. Other workers[8,10] have achieved monocrystalline ZnSe growth by vacuum evaporation most readily on (100), with difficulty on (110), and not at all on (111), suggesting that our films may be faceting to the preferred (100) plane. Monocrystalline CdSe has been reported on both the (100)[11] and the (111)[12] planes, but surface smoothness was not discussed. On the other hand, monocrystalline ZnTe has been reported obtainable on (111) but not on (100).[13] Figure 3 is the LEED pattern of film No. 3 and is typical of patterns from films classified as "well-ordered epitaxial". The

hexagonal array of bright, sharp diffraction beams indicates a well-ordered single-crystal film of ZnSe oriented in the (111) plane of the cubic system, which is identical to the (0001) plane of the hexagonal system. Also faintly visible are some beams halfway between the bright beams and the center of the hexagon, and halfway between adjacent bright beams. This is a so-called half-order array indicative of a surface structure having twice the bulk lattice period; it is often observed on II-VI surfaces. The large white area is a reflection.

Figures 8a-f are the Auger spectra of the various films grown in this work. Relative elemental peak heights for the binary films were always reproducible to within the $\pm$10% accuracy of the technique, so that no gross deviations from stoichiometry were ever observed. Compositions reported for the ternary films were calculated from the Auger spectra by linear interpolation between the limiting binary spectra.

E. Waveguide Measurements

6328Å light has been coupled into several ZnSe films using a clamped-on rutile prism and into a ZnTe film using a taper-coupler grown into the film by employing a knife-edge mask during growth. These films are indicated in Table III. A 2 mm streak was observed in a ZnSe film on sapphire which the vendor had supplied 30° off the desired (0001)

orientation (No. 7). Seven TE modes, with the lowest mode having a 5 mm-long streak, were observed in a ZnSe film on CaF_2(111) (No. 5). From coupling angle measurements on the latter film we calculated the film's bulk index of refraction to be 2.58 and its thickness to be 1.62 microns, agreeing closely with the known ZnSe index of 2.58 at 0.633 microns[15] and the interferometrically-measured film thickness of 1.68 microns. Two TE modes were observed in film No. 4, ZnSe on CdS, but were discernable only by a glow at the prism corner, indicating very high losses. Again, index and thickness calculated from coupling angles (2.5812 and 0.69 microns) agreed closely with known values. All three of these films were polycrystalline, although mirror-smooth. Presumably, therefore, the high propagation losses were due predominantly to scattering from crystallite interfaces. The fact that losses are higher for the film on CdS than for those on CaF_2 or sapphire may mean smaller crystallites in the latter cases, providing more nearly amorphous, isotropic conditions. Amorphous optics generally exhibit lower losses than do polycrystalline ones.

A 5 mm streak was observed in a film of ZnTe on CaF_2 (No. 19), as reported in October. Although the hexagonal mosaic of cracks suggests some degree of crystallographic ordering, the extent of that ordering is difficult to assess without LEED observation. The relatively high propagation losses suggest numerous grain boundaries.

Bulk scattering losses from single-crystal films are expected to be considerably lower than those observed above on polycrystalline films. Unfortunately, the single-crystal films grown in this work either were too thin or had surfaces too rough to permit coupling. It was determined that none of the films grown were of sufficient quality to make worthwhile further propagation measurements in the more difficult infrared region.

IV. CONCLUSIONS AND RECOMMENDATIONS

Films of II-VI compounds were grown in this work in a system incorporating state-of-the-art ultra-high vacuum technique to eliminate contamination and a variety of monitoring techniques to achieve the best possible process control. They were grown on substrates having high surface and crystallographic quality and having near-optimum physical constants. The fact that, despite this, films having both good crystallographic and good surface quality could not be obtained would seem to imply that a more fundamental restriction is coming into play. Possibly, the desired film will grow only on a crystallographic plane which has not yet been tried. Or possibly, the high volatility of the group II and VI elements requires that growth be carried out at much higher pressures (i.e., not by MBE), to approach more closely an equilibrium situation.

Further work should be done to determine the effect of the substrate crystallographic orientation. Recently reported liquid-phase epitaxial growth of ZnTe on ZnSe[16] has resulted in good films on (111B) and poor ones on (111A), (110), and (100). The (0001A) planes of the hexagonal substrates, equivalent to the (111A) plane of a cubic film, were used in this work because higher quality polished surfaces were obtained than on (0001B). This problem is being o ercome, and the (0001B) face should be tried next.

Reported ZnSe growth work[8-10] has indicated that (100) is the preferred orientation. Scanning electron microscope examination of single-crystal films grown in the present work may reveal if our films have faceted to (100) or to another plane. Growth on planes other than (0001) involves two complications, however, which had originally led us to the decision to concentrate our efforts on that plane. First, the electro-optic effect is strongest when the field is perpendicular to and the guide parallel to the (0001) plane. The (110) plane is somewhat less desirable. The (100) is least desirable both because the effect is weakest and because it is dependent on the direction of propagation in the film, although these effects are not serious enough to rule out (100). Second, only CdS and CdSe are presently available in large (>1cm) single-crystal bulk ingots of sufficiently high quality. They are both of hexagonal symmetry, while the films to be grown are generally cubic, and only the (0001) plane has a matching plane (the (111) plane) in the cubic system. Cubic ZnSe is just now becoming available, and this should be tried. A number of cubic III-V semiconductors are available, and these would probably make good substrates, except that their indices of refraction are higher than for the II-VI compounds. Consequently, it would be necessary to grow a rather thick II-VI cladding under the guide to prevent absorption of the evanscent field by the substrate, but this is a possibility.

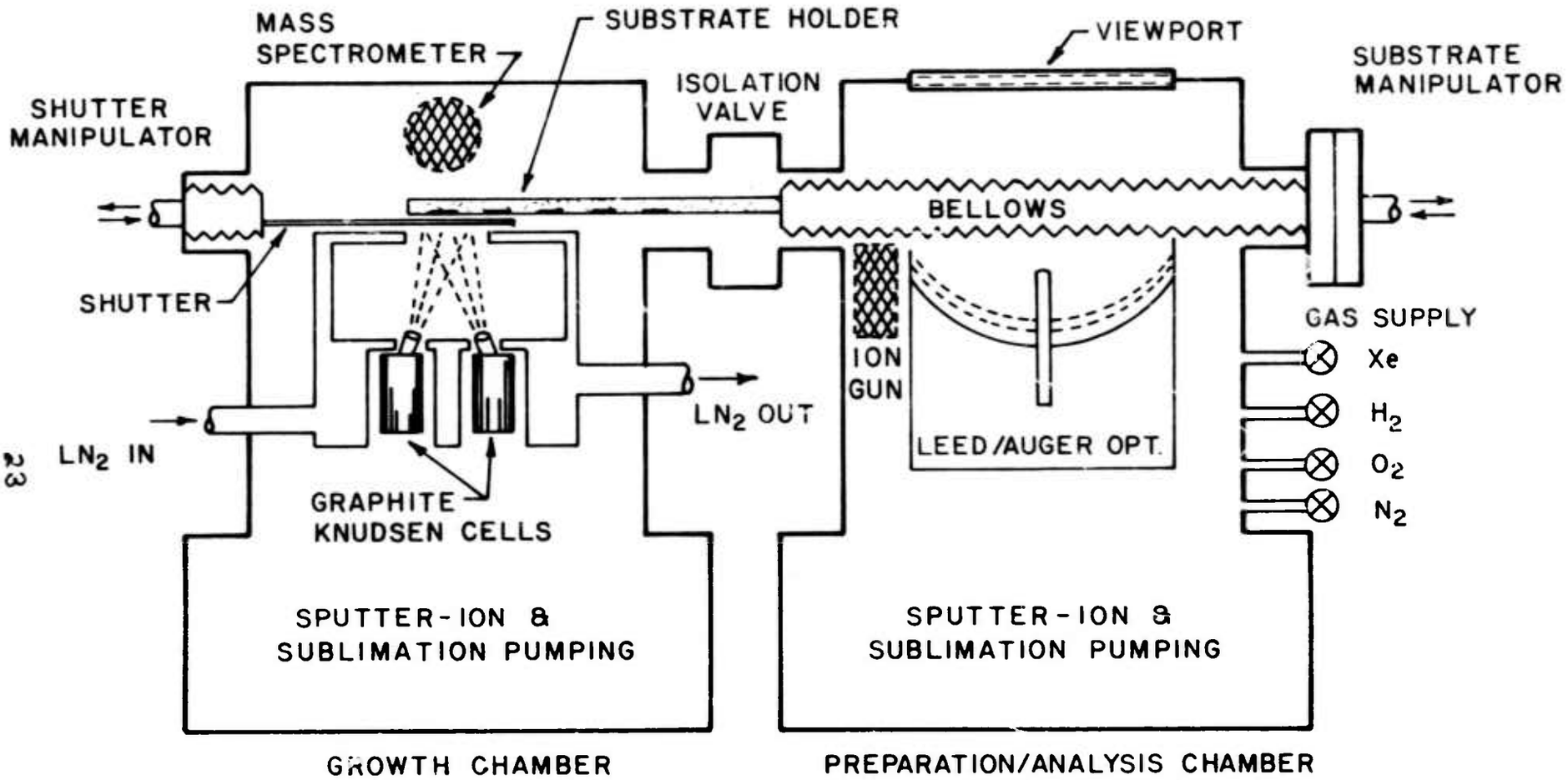

FIG. 1. SCHEMATIC OF MBE SYSTEM

FIG. 2. LEED PATTERN OF CdSe (0001)
SUBSTRATE AT 52 eV

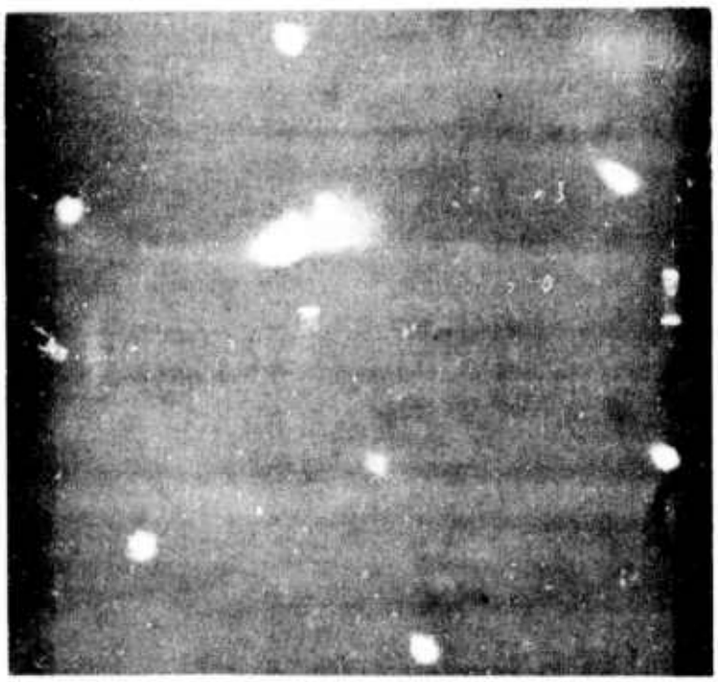

FIG. 3. LEED PATTERN OF ZnSe (111)
FILM AT 35 1/2 eV

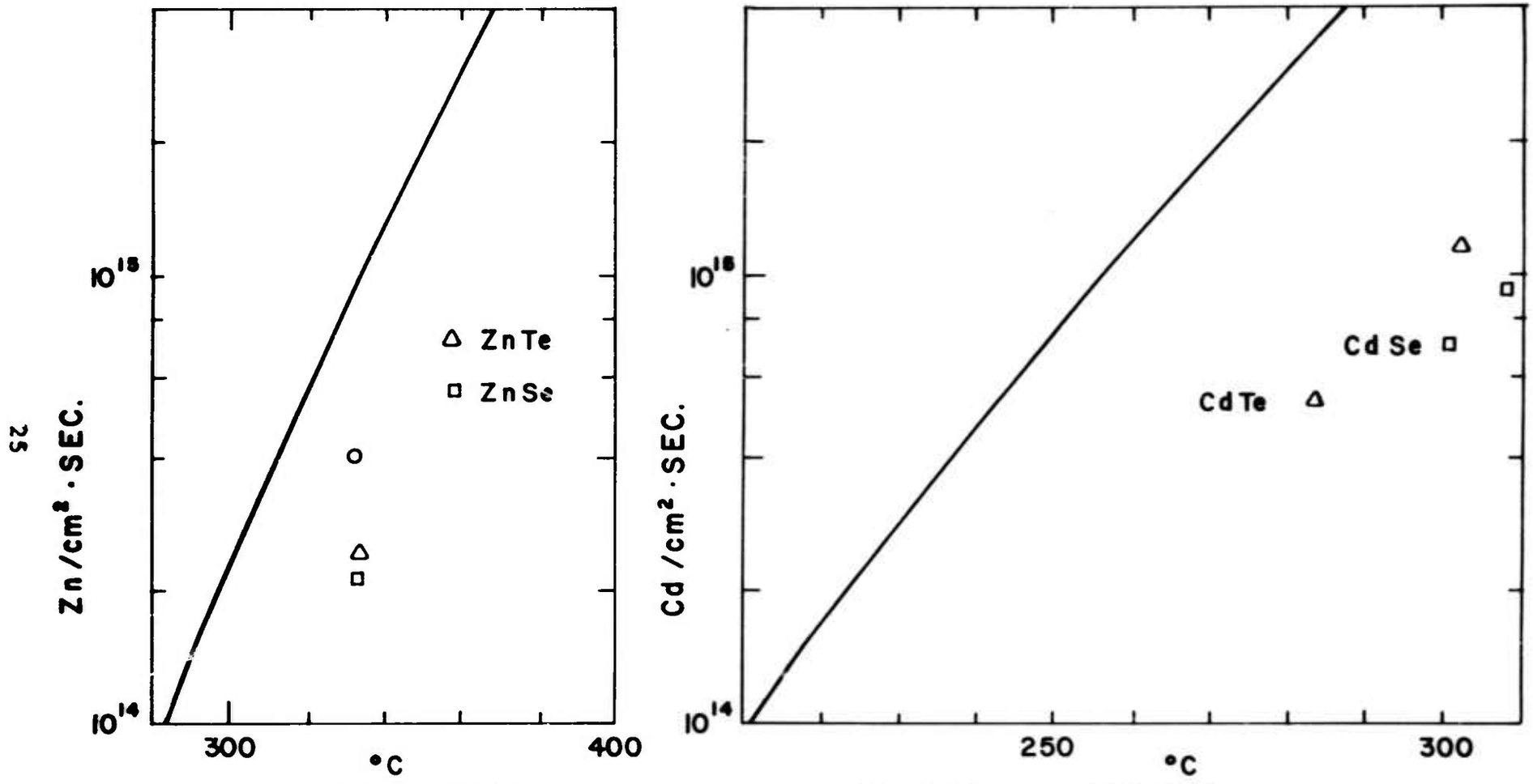

FIG. 4 ELEMENTAL IMPINGEMENT RATE CALIBRATIONS
(AT 5cm. FROM CELL ORIFICE)

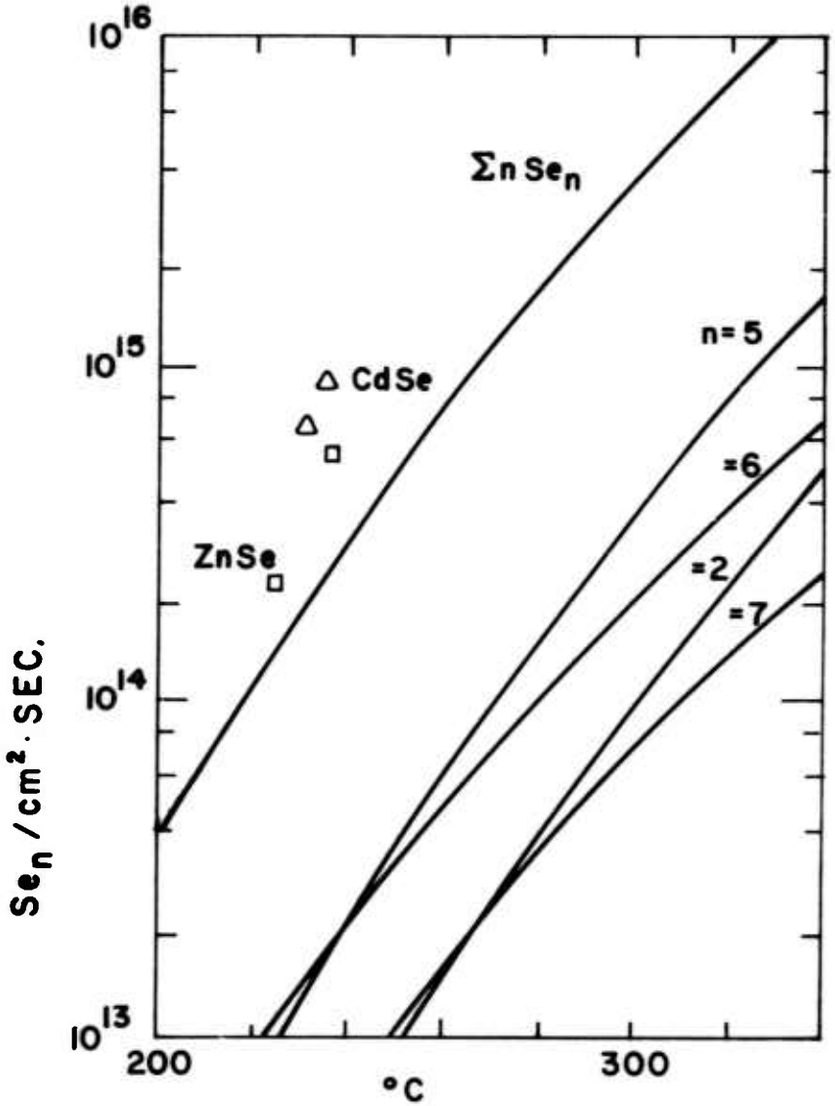

c. Se (1 mm ORIFICE)

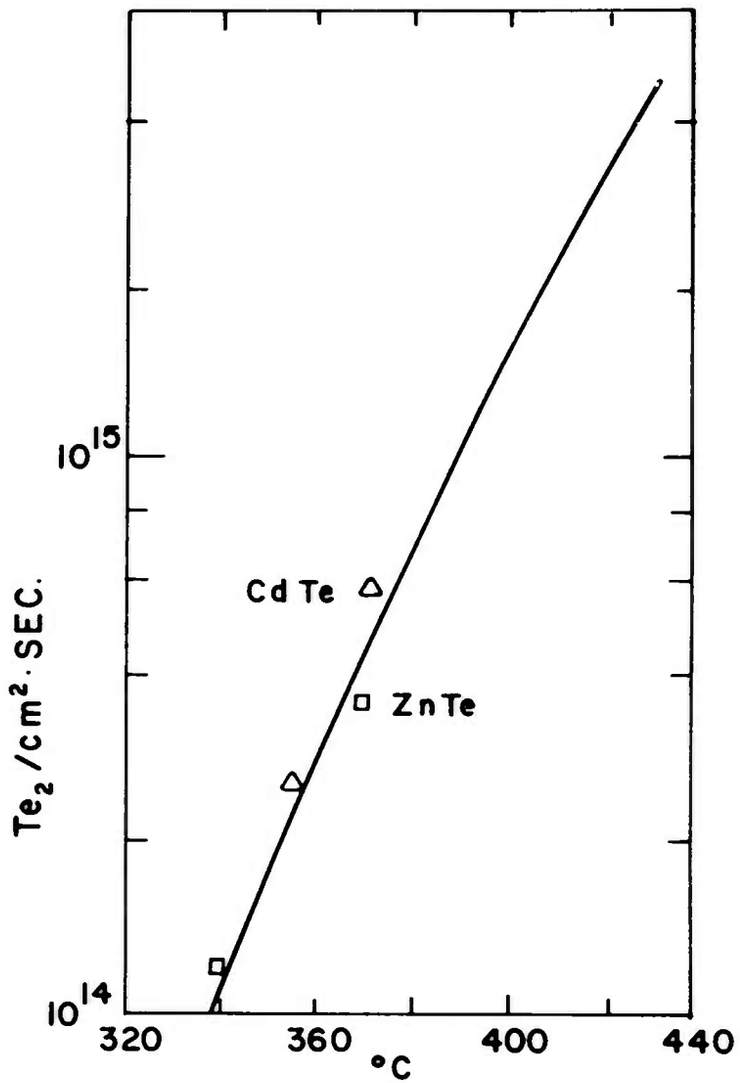

d. Te (3 mm ORIFICE)

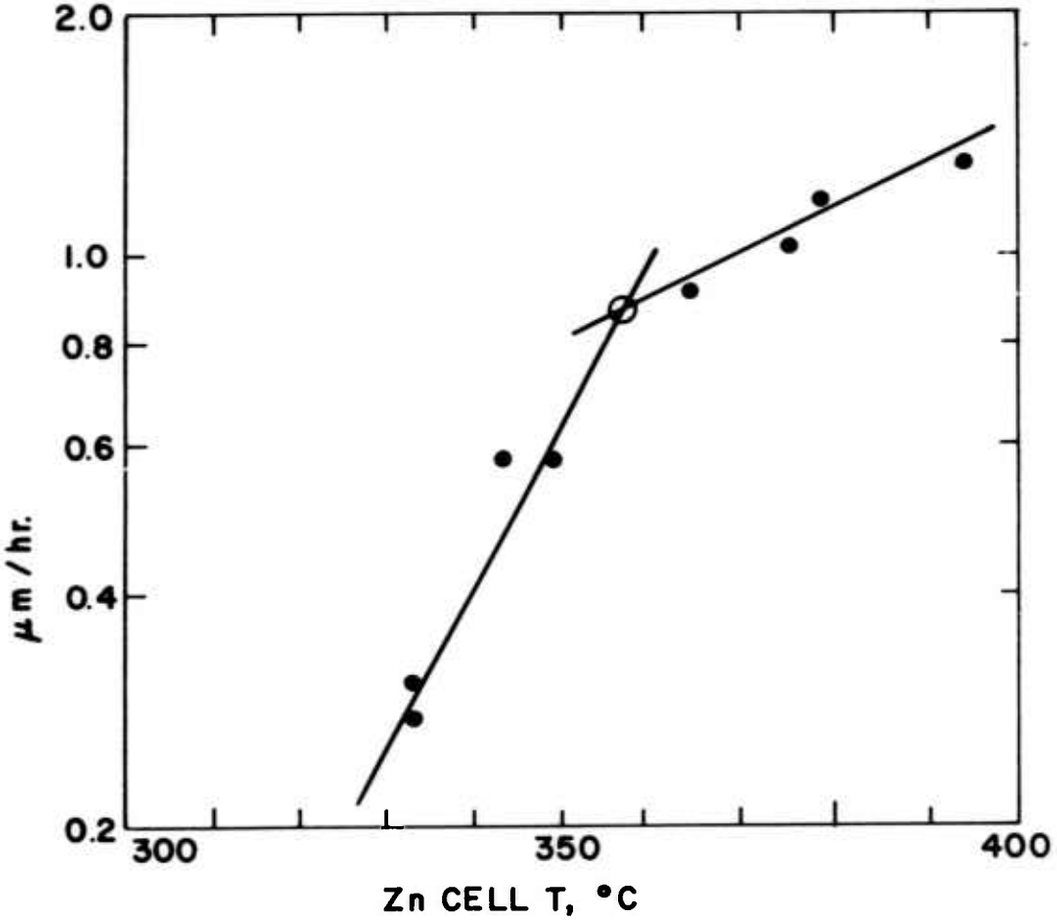

a. Zn Se (Se CELL T=236 °C)

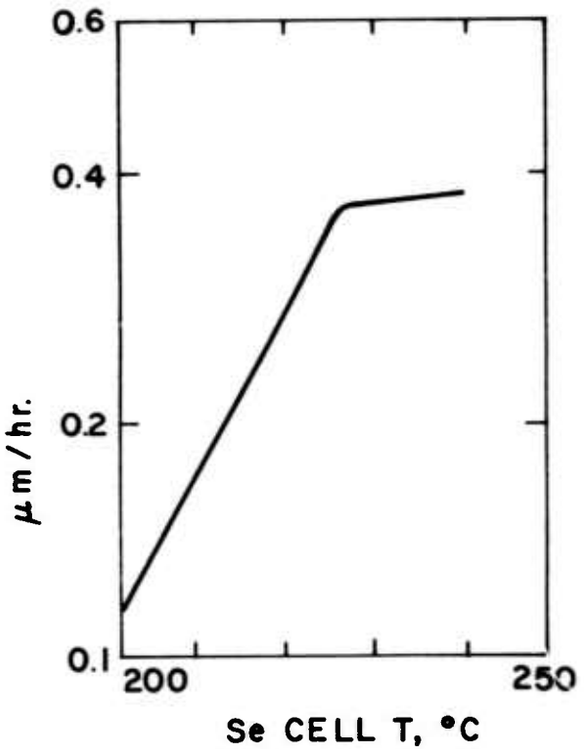

b. Zn Se (Zn CELL T=333 °C)

FIG. 5. II-VI COMPOUND GROWTH RATES MEASURED BY QUARTZ CRYSTAL AS FUNCTIONS OF KNUDSEN CELL TEMPERATURES

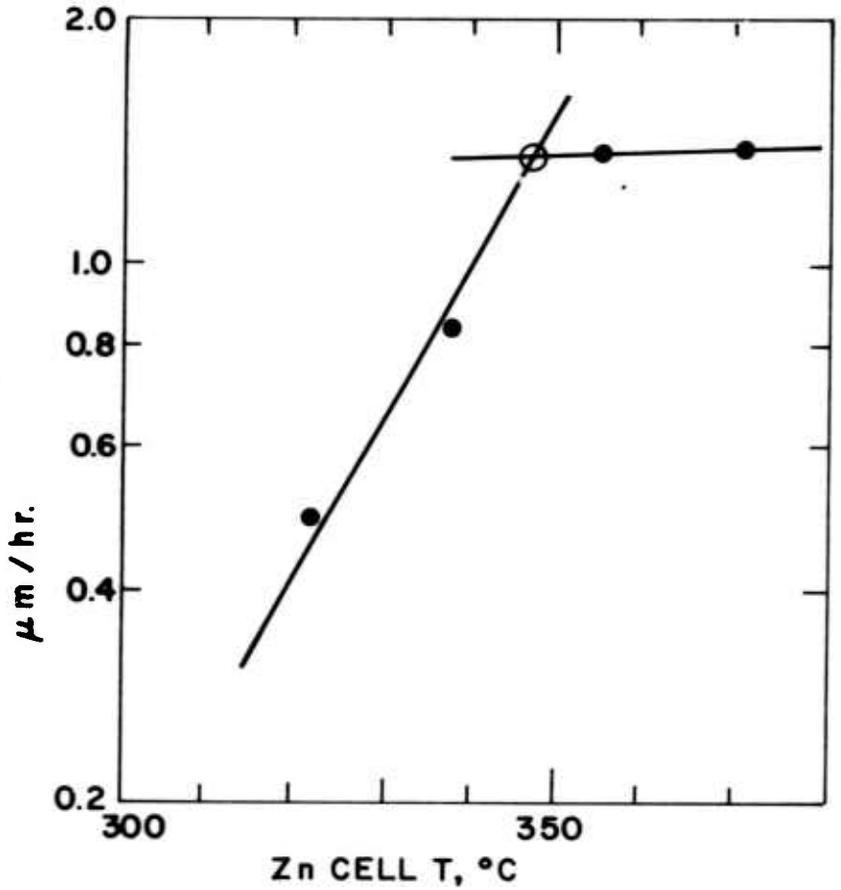

c. Zn Te (Te CELL T=368°C)

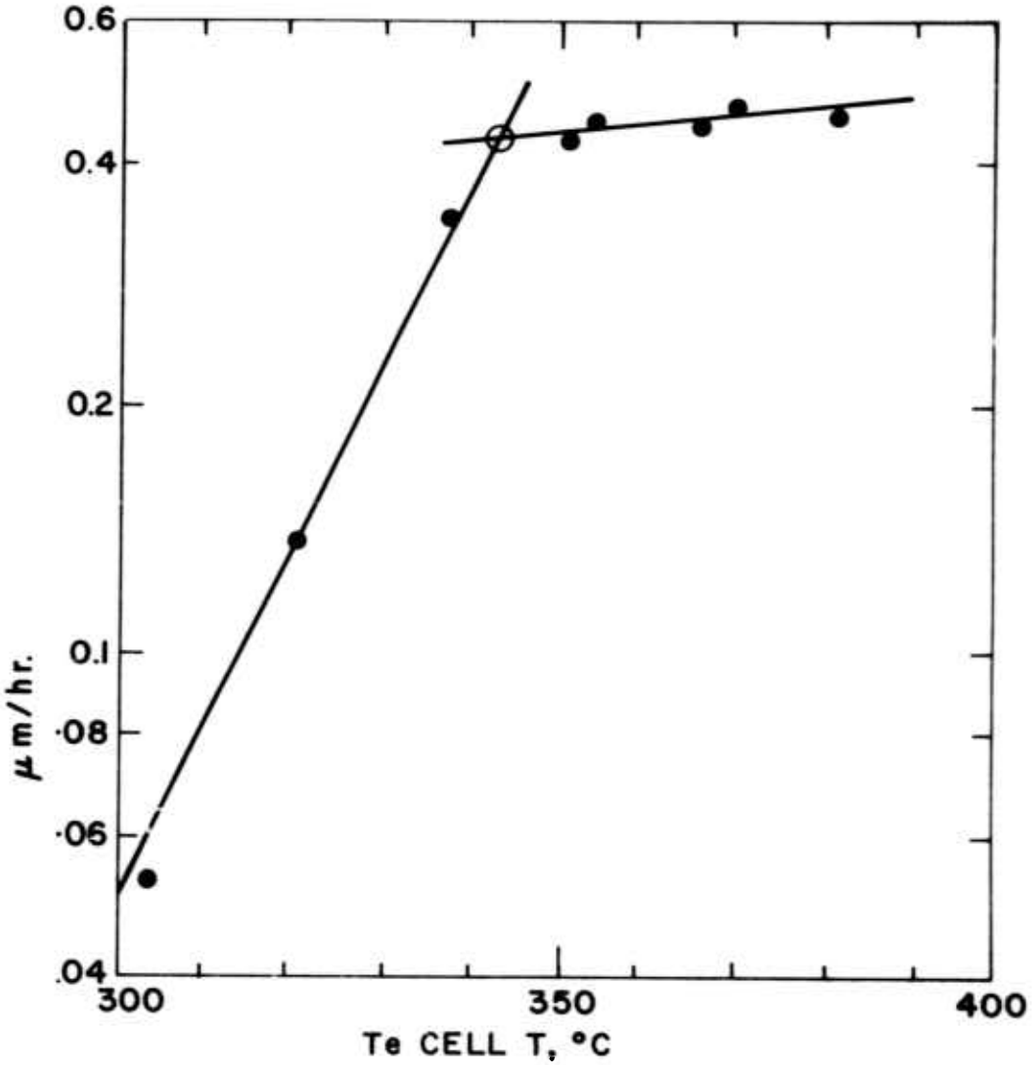

d. Zn Te (Zn CELL T= 333°C)

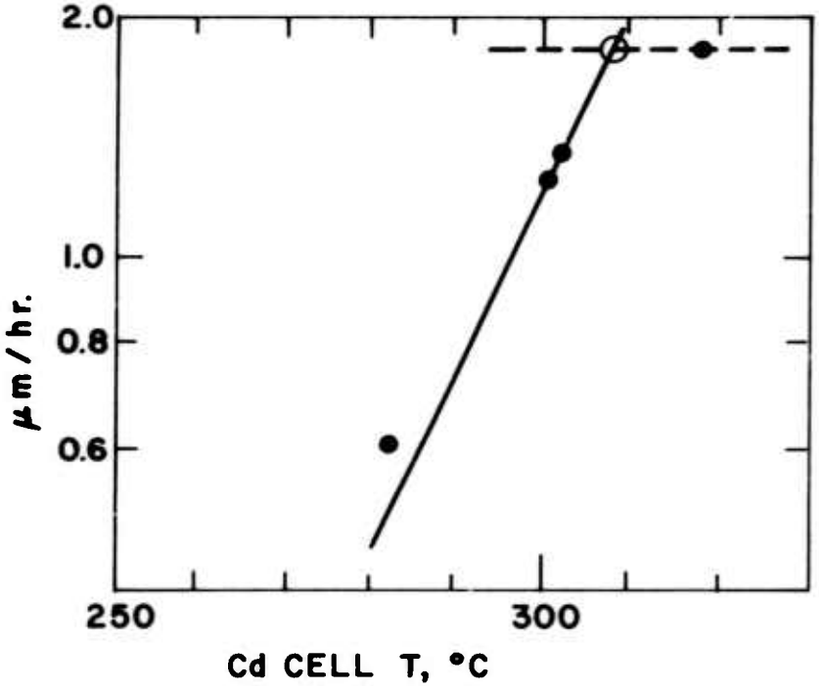

e. CdSe (Se CELL T=236°C)

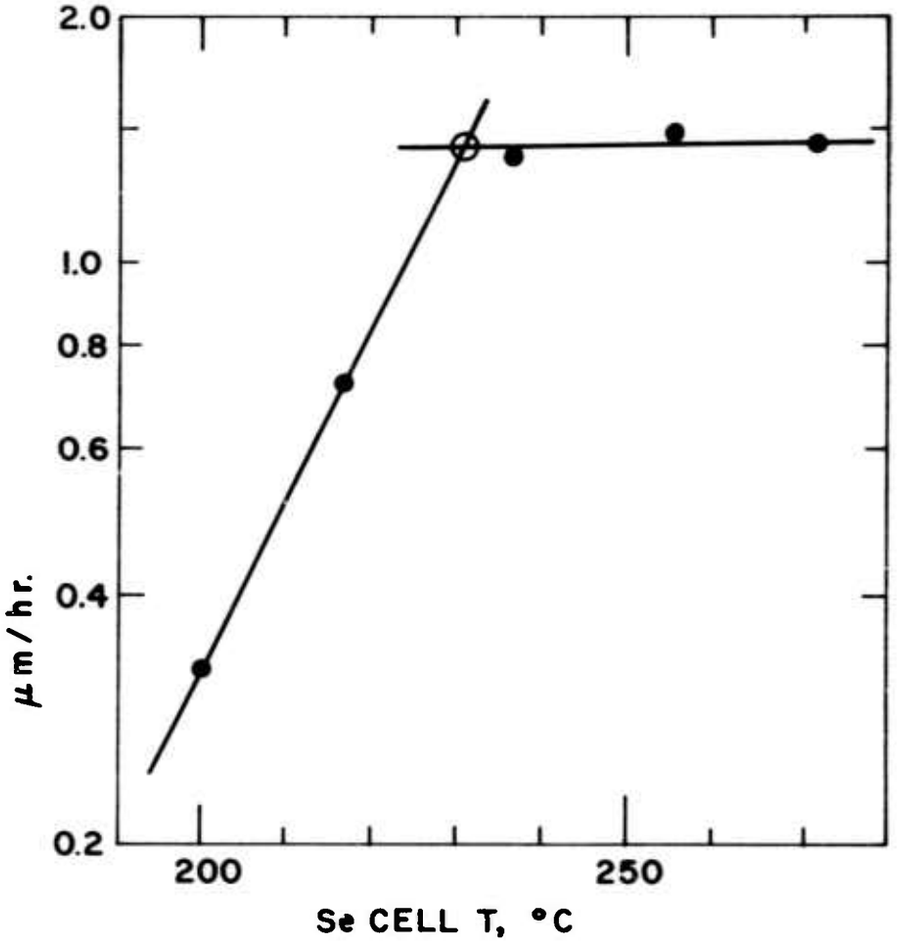

f. CdSe (Cd CELL T=301°C)

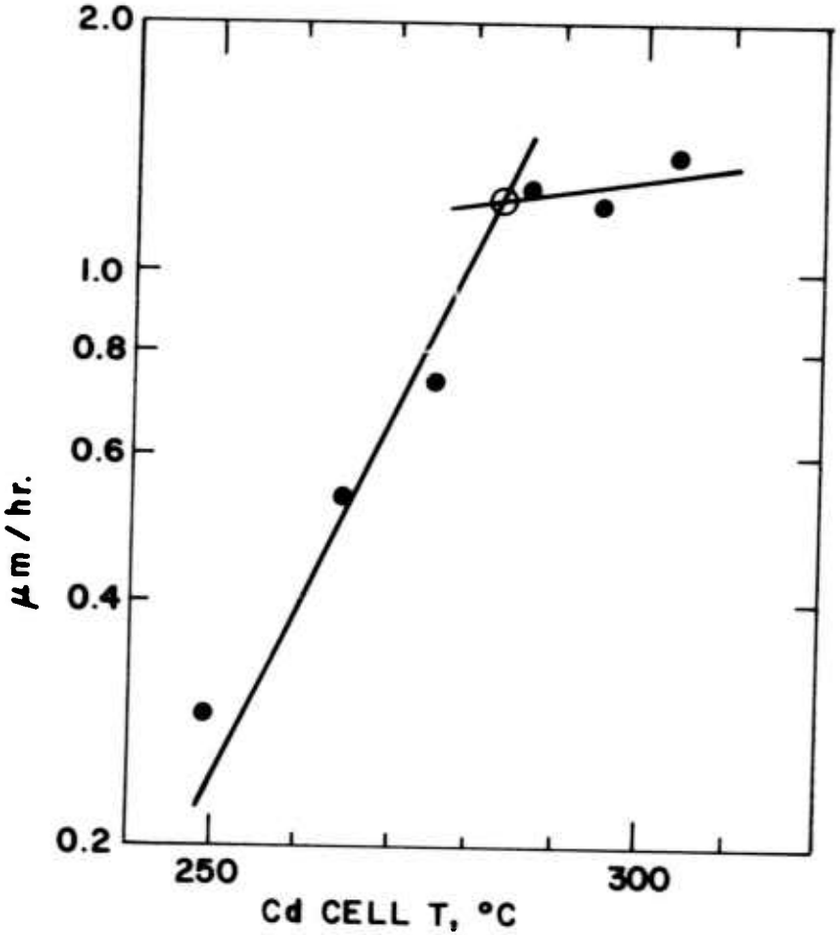

g. Cd Te (Te CELL T= 355 °C)

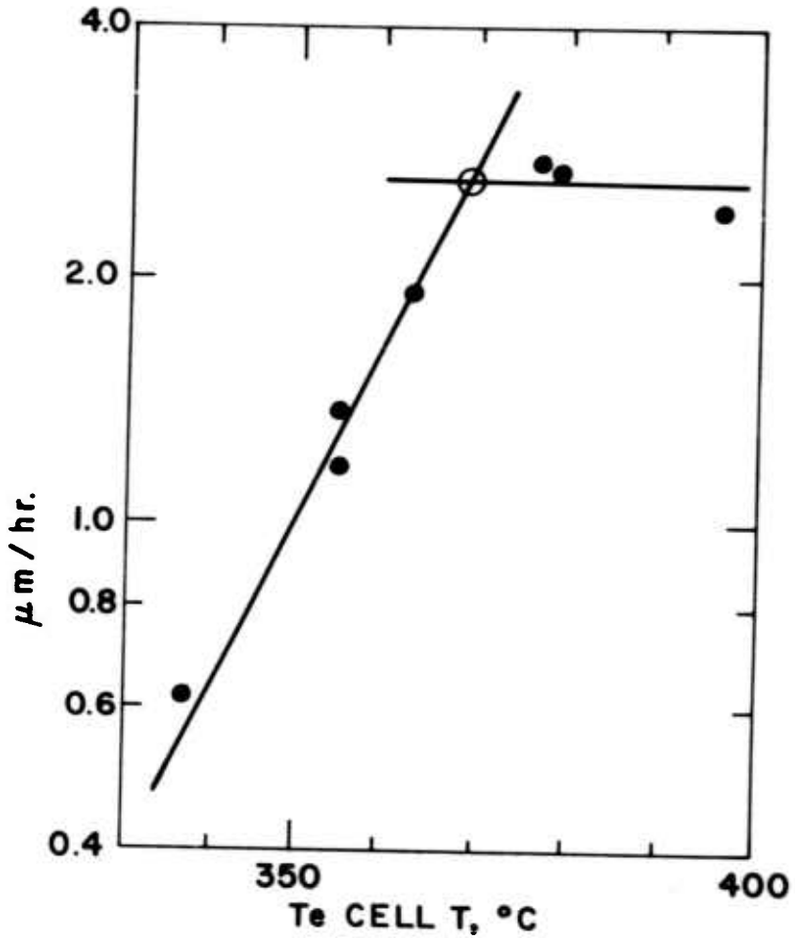

h. Cd Te (Cd CELL T= 302 °C)

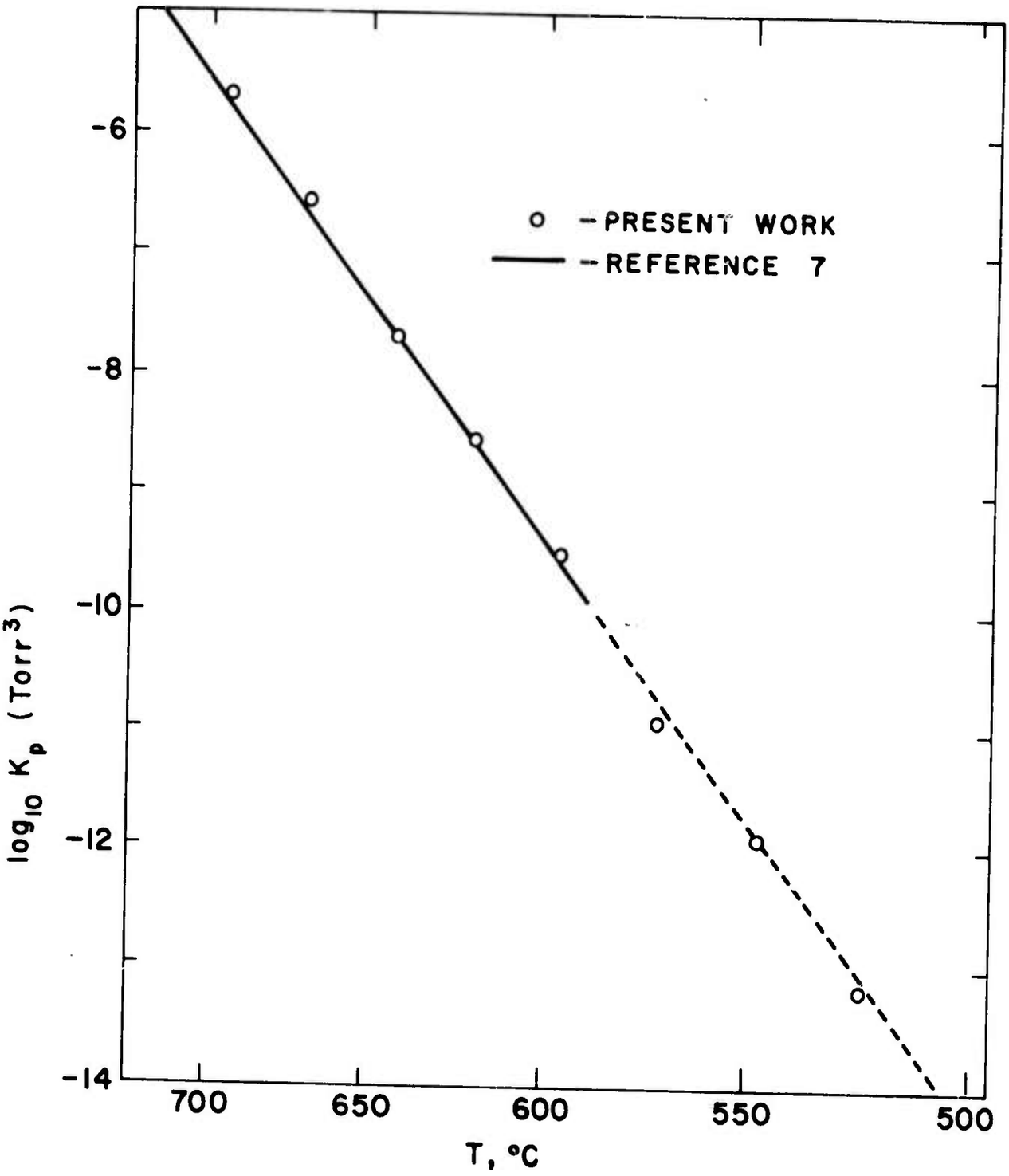

FIG. 6. EQUILIBRIUM CONSTANT FOR ZnTe EVAPORATION

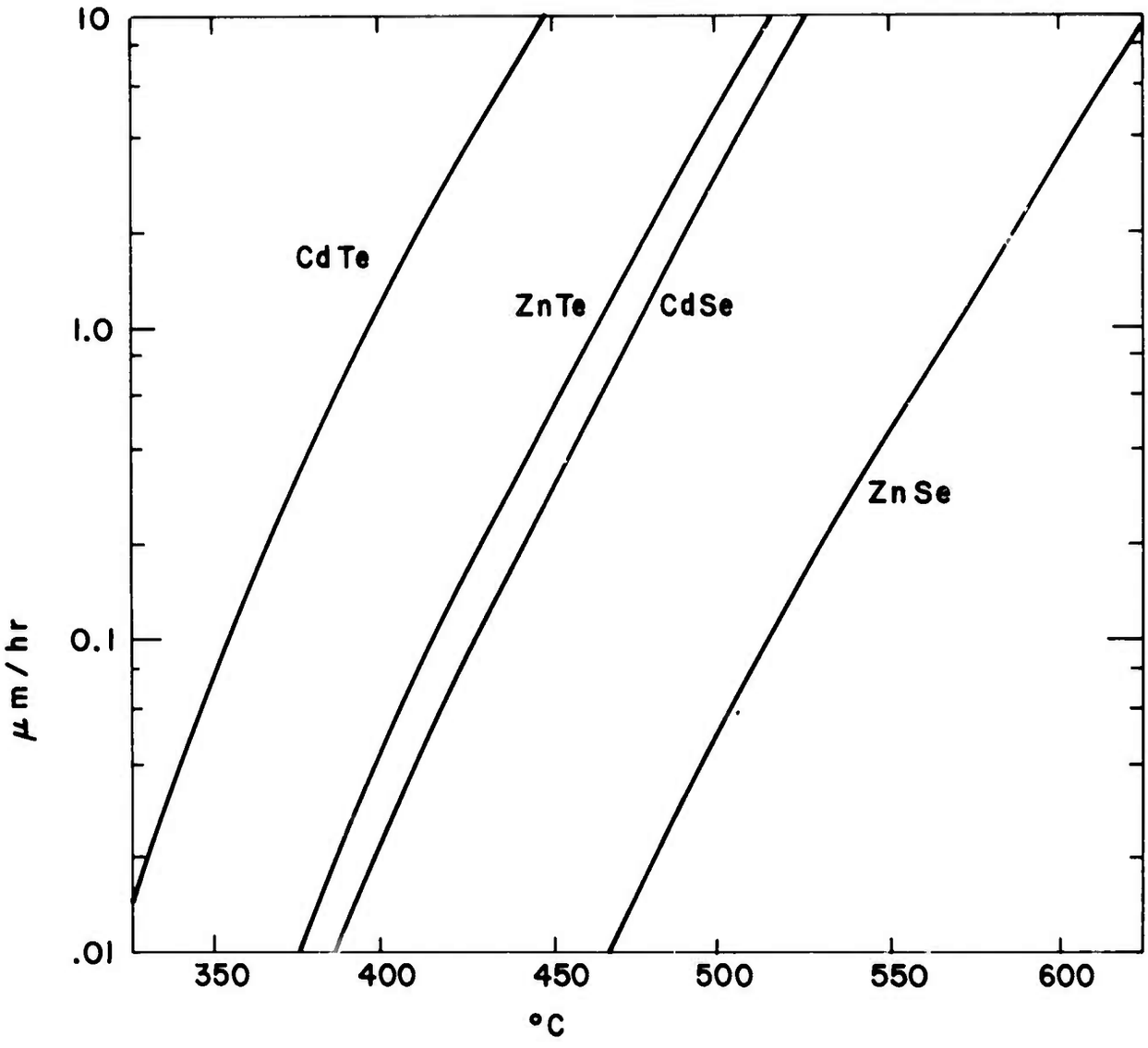

FIG. 7 II-VI COMPOUND EVAPORATION RATES

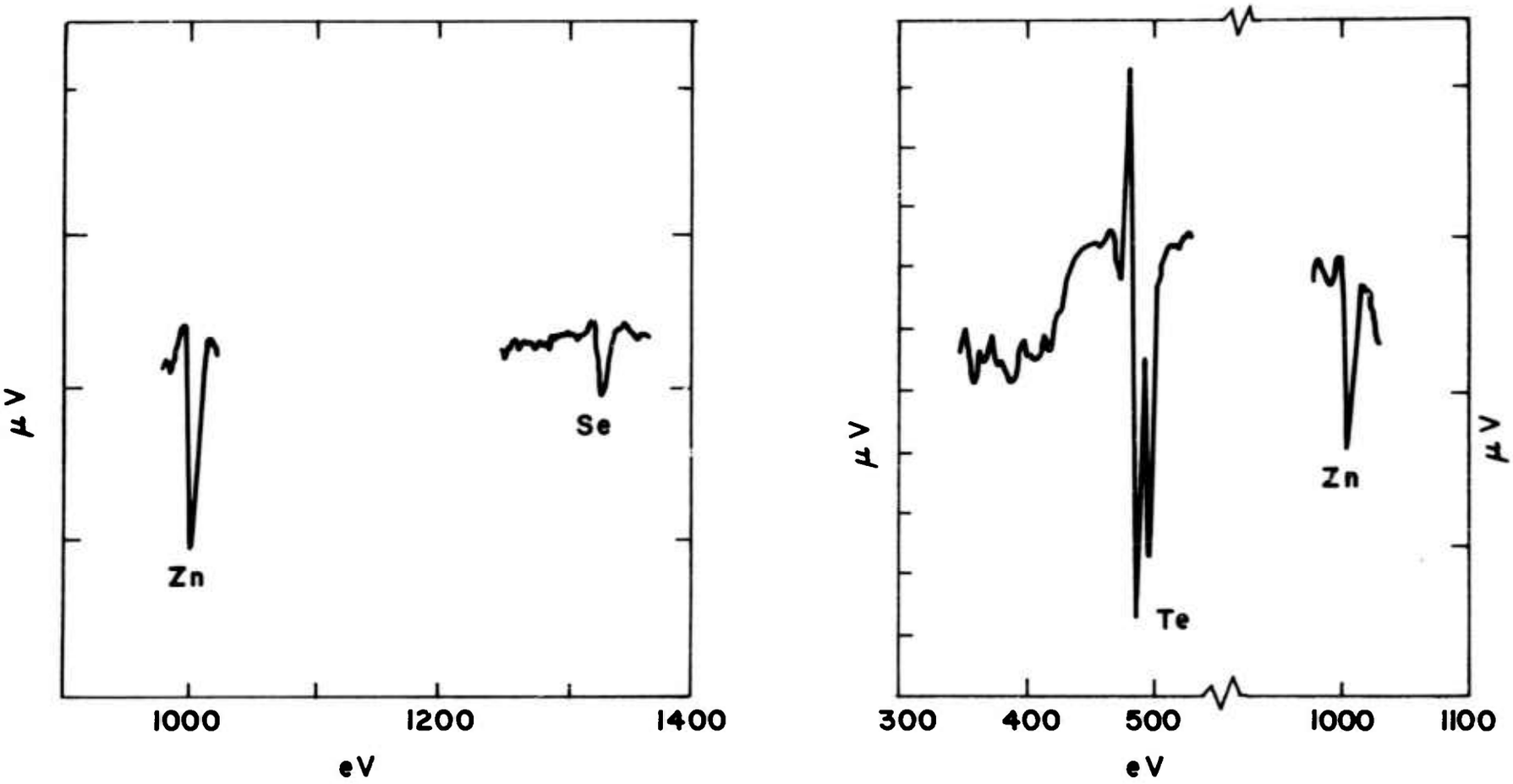

FIG. 8. AUGER SPECTRA OF GROWN FILMS

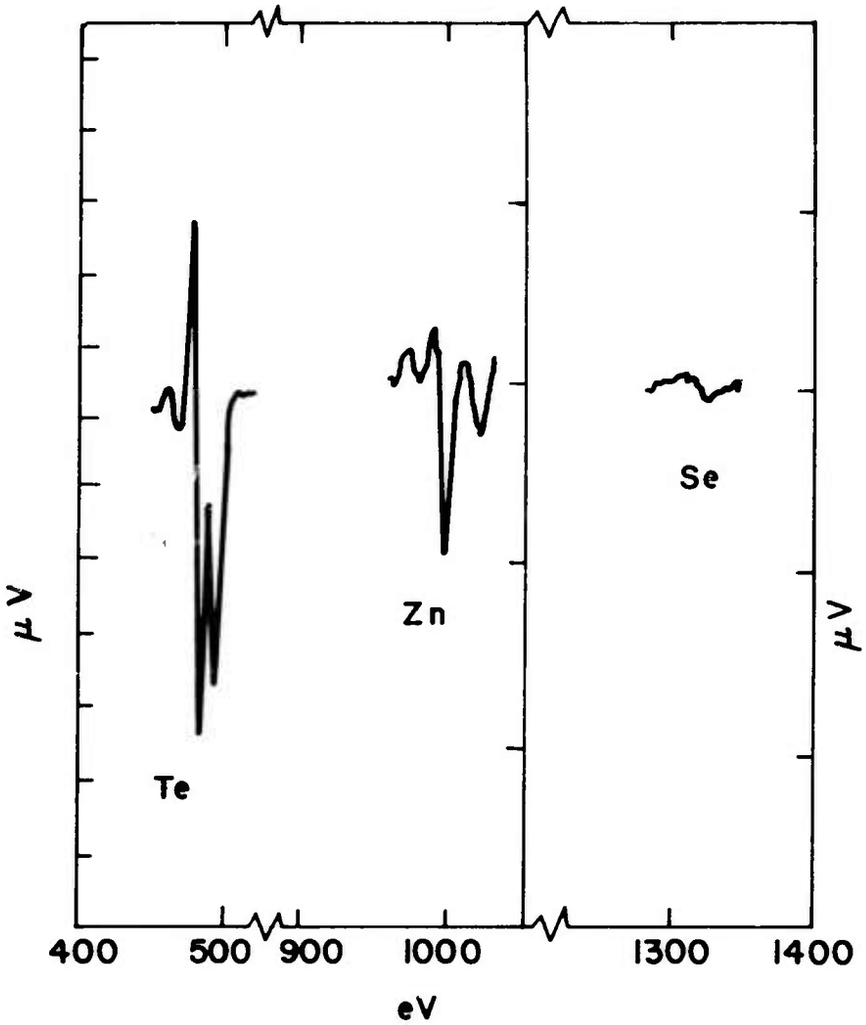

c. $ZnSe_{.24}Te_{.76}$

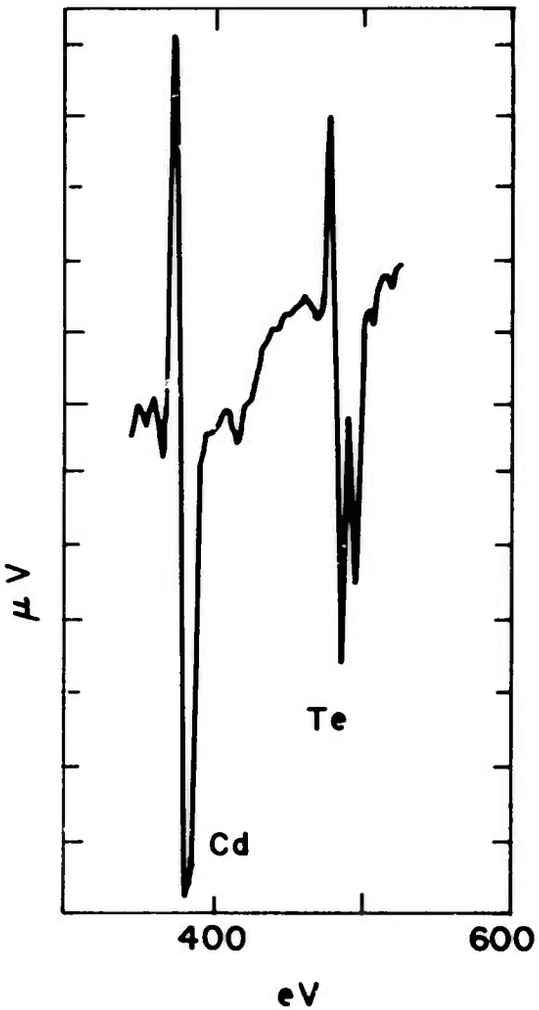

d. Cd Te

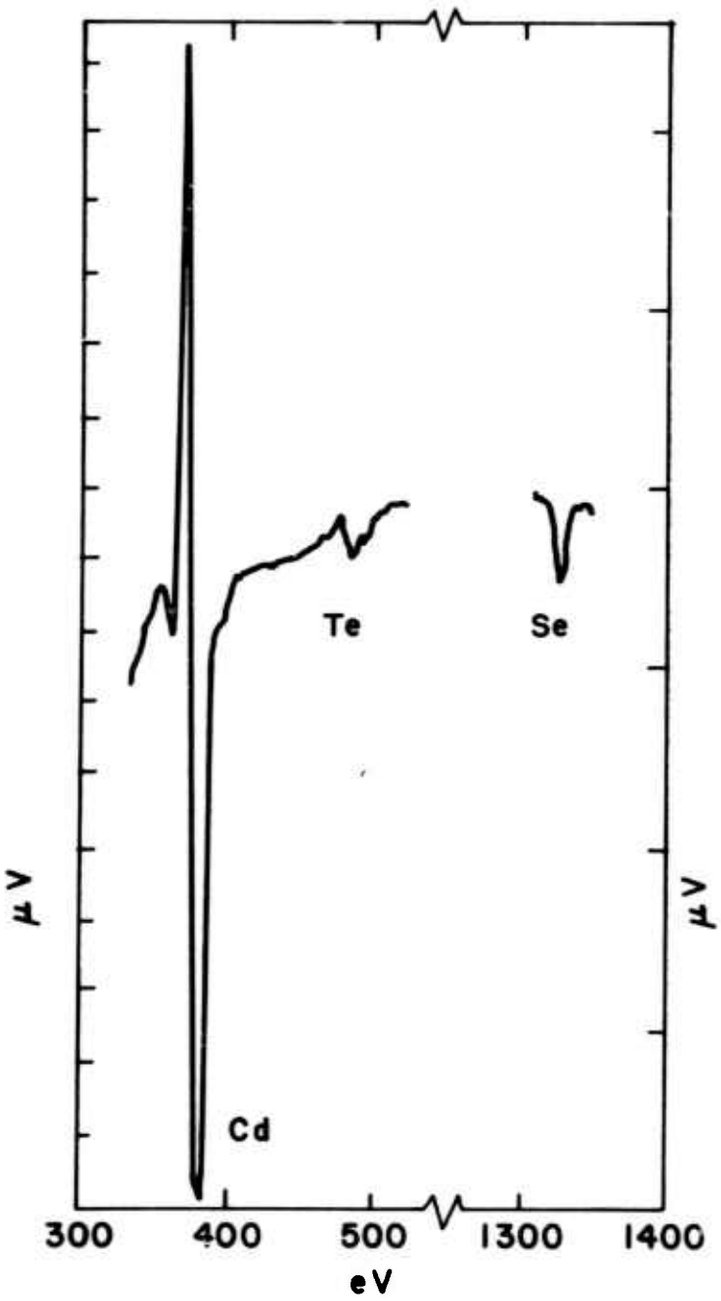

e. $CdSe_{.95}Te_{.05}$

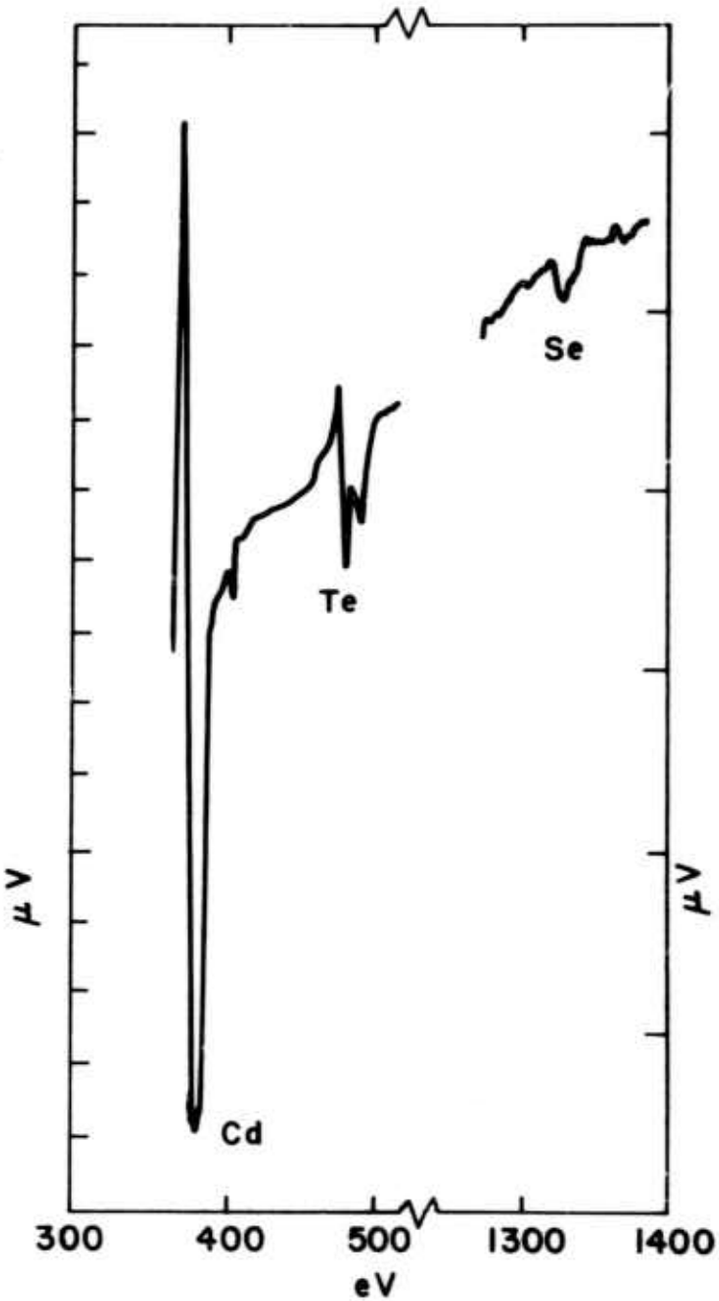

f. $CdSe_{.7}Te_{.3}$

TABLE I

Specifications of Source Materials

Composition	Source	Specified purity, nines
Zn	Cominco	6
Cd	Cominco	6
Se	Alfa	4
Te	Cominco	6
ZnTe	Eagle-Picher	5

Compound	Molecular Weight amu	Density, $\frac{\text{grams}}{\text{cc}}$	$\frac{\text{Molecules}}{\text{cc}}$	$\frac{\text{Molecules/cm}^2\text{.sec.}}{\text{microns/hr}}$
ZnSe	144	5.42	2.26×10^{22}	6.3×10^{14}
ZnTe	193	6.34	1.98×10^{22}	5.5×10^{14}
CdSe	191	5.81	1.83×10^{22}	5.1×10^{14}
CdTe	240	6.20	1.55×10^{22}	4.3×10^{14}

TABLE II

Physical Constants of II-VI Compounds

TABLE III - Characteristics of Grown Films

Film No.	Film Comp.	Substrate	Growth T°C	Imping. rate, microns/hr	Thick-ness, microns	Sticking Coeff.	Visual appear.*	LEED interp.**	Wave-guiding observed	delivered to NRL	Comments
1	ZnSe	CdS(0001A)	450	3	0.26	0.3	2	2f			
2			418	3	0.46	0.4	2	3			
3			425	1	.08	.08	1	1		X	LEED photo Fig. 3
4			375	1	0.65	0.7	1	3	X	X	
5			300	1	0.71	0.7	1	3			
6		CaF_2(111)	300	1	1.68	1.0	1		X	X	
7		sapphire	300	1	2.52	1.0	1		X	X	Misoriented substrate
8	ZnTe	CdSe(0001A)	350	5	5.8	1.0	3	2		X	
9	$ZnSe_{.24}Te_{.76}$		400	2	1.68	1.0	1	3		X	
10	ZnTe		350	2	1.15	1.0	2	3		X	
11	$ZnSe_{.24}Te_{.76}$		350	2	0.87	1.0	1	3		X	
12	ZnTe	CdS(0001A)	400	1	.09	.09	1	1			
13			400	1	.07	.07	2	1			
14			400	1	.07	.07	1	1			
15			350	1	.09	.09	2	1-2			
16			300	1	0.44	0.4	1	3		X	
17		CaF_2(111)	450	1	1.50	1.0	2				Initiate growth at 350°C cracked to hexag. mosaic
18			350	1	2.50	1.0	1				cracked to random mosaic
19			350	1	1.10	1.0	1		X		cracked to hexag. mosaic
20	$CdSe_{.95}Te_{.05}$	CdSe(0001A)	350	1	0.19	0.2	3	1		X	
21	$CdSe_{.7}Te_{.3}$		300	1	0.69	0.7	3	2		X	
22	CdTe		300	2	0.56	0.4	1	2		X	
23			350	1	.08	.09	1	1			
24			300	1	0.30	0.3	3	1		X	

* 1- mirror-smooth, 2-hazey, 3-coarse and grainy
** 1- well-ordered epitaxial film, 2- some ordering, 3- polycrystalline/amorphous, f- faceting observed

REFERENCES

1. R. E. Honig and D. A. Kramer; RCA Review 30 285 (1969)
2. W. J. Moore; "Physical Chemistry", Prentice-Hall, Englewood Cliffs, N. J. (1962); p. 217.
3. J. Berkowitz and W. A. Chupka; J. Chem. Phys. 48, 5743 (1968)
4. A. Y. Cho; J. Vac. Sci. and Tech. 8, S31 (1971)
5. L. L. Chang, L. Esaki, W. E. Howard, and R. Ludeke; J. Vac. Sci. and Tech. 10, 11 (1973)
6. K. Denbigh; "The Principles of Chemical Equilibrium" University Press, Cambridge, U. K. (1963); p. 144
7. P. Goldfinger and M. Jeunehomme; Trans. Faraday Soc. 59 2851 (1963)
8. J. E. Genthe and R. E. Aldrich; Thin Sol. Films 8, 149 (1971)
9. J. T. Calow, D. K. Kirk, and S. J. T. Owen; Thin Sol. Films 9, 409 (1972)
10. J. T. Calow, S. J. T. Owen, and P. W. Webb; Phys. Stat. Sol. 28, 295 (1968)
11. L. A. Sergeyeva, T. P. Kazannikova, I. A. Kharlamov and V. B. Aleskovsky; Thin Sol. Films 11, 105 (1972)
12. R. Ludeke and W. Paul; Phys. Stat. Sol. 23, 413 (1967)
13. D. B. Holt; Brit. J. Appl. Phys. 17, 1935 (1966)

References cont.

14. E. P. Warekois, M. C. Lavine, A. N. Mariano, and H. C. Gatos; J. Appl. Phys. 33, 690 (1962)

15. D. B. Hall, "Integrated Optical Circuits", rpt. # NELC/TR-1861, Naval Electronics Laboratory Center, San Diego (1973); p. 5

16. S. Fujita, F. Moriai, S. Arai, and T. Sakaguchi; J. Appl. Phys., 12, 1841 (1973)

CHEMOMECHANICAL POLISHING OF CdS

Vincent Y. Pickhardt and Donald L. Smith

Perkin-Elmer Corporation, Norwalk, Connecticut 06856

ABSTRACT

The chemomechanical polishing of the "A" or cadmium-rich face of cadmium sulfide has been accomplished. The etchant contained 90 ml nitric acid, 300 ml precipitated silica and 10 g aluminum chloride per 1000 ml water. Best results were obtained using a poromeric polishing disk with 370 g/cm^2 work pressure at 240 RPM polishing wheel speed. Surfaces were completely featureless when viewed by Nomarski and Michelson interference microscopy at 155 and 400x, and gave good LEED patterns after brief heat-cleaning under vacuum.

CHEMOMECHANICAL POLISHING OF CdS

Vincent Y. Pickhardt and Donald L. Smith

Perkin-Elmer Corporation, Norwalk, Connecticut 06856

CdS is a desirable substrate for the epitaxial growth of semiconductor thin films for electro-optic devices. For such applications, the crystals must be flat, highly polished and damage-free. Many etchants have been suggested in previous articles (1-3), but none of them produces all of these surfaces requirements simultaneously. We describe below a procedure utilizing both mechanical and chemical polishing which produces excellent results on the (0001A) face of CdS.

EXPERIMENTAL PROCEDURE

Undoped, single-crystal CdS (Eagle-Picher ultra-high purity grade) was x-ray oriented to within 2^{o} of the (0001) plane and sawn by a continuous loop wire saw into 8x10x2 mm wafers. The "A" face was differentiated from the "B" face by a 60 second etch in 50%* HCl(1). The oriented crystals were mounted on a 3cm-diameter titanium polishing block with the

* All concentrations of HCl and HNO_3 are expressed as a volume percent of the standard 38% and 70% assay solutions respectfully.

"A" face exposed. A schematic of the equipment is shown in Figure 1. The block and its closely-fitting dressing ring are held by rollers about half-way out to the edge of the 10-inch diameter motor-driven polishing pad, and the block and ring rotate about their axis due to friction with the pad, providing compound motion.

The wafers were first mechanically polished on a 3-micron silicon carbide-impregnated polishing disk with water as lubricant, to remove all surface and subsurface wire saw damage. Both polishing block and dressing ring were then cleaned in a concentrated detergent to remove any particle contamination. Final chemical polishing was completed on the same apparatus. The etchant which produced best results contained 90 ml HNO_3, 300 ml precipitated silica, 10g $AlCl_3$ (anyhdrous powder) and 1 ml concentrated detergent as an anticoagulant per 1000 ml deionized water. This was fed to the polishing pad immediately after mixing at approximately 25 ml/min. The crystals were weighted to 370 g/cm^2. Best results were obtained using a Politex-Pix poromeric polishing pad at a speed of 240 RPM.

RESULTS

After approximately 30 minutes of polishing with the above etchant, the crystal surfaces showed a flat, highly polished, "mirror-like" finish. Surfaces were completely

featureless when viewed by Nomarski microscopy at 155 and 400 x. When viewed by Michelson interference microscopy at 370 x the crystals showed no defects and showed flatness to better than 300Å (resolution limit) over the 0.3 mm field.

Of upmost importance is removal of all subsurface damage from sawing and mechanical polishing operations. Although a polishing time of 30 minutes is suggested, in some instances this must be lengthened to remove preferential etching caused by leftover subsurface damage. Extreme care must be taken while handling crystals so as not to introduce damage between operations. The etchant composition is also important. An increase in acid concentration produces large etch pits, a decrease in concentration produces surface "scratching". Deletion of $AlCl_3$ produces preferential etching and surface "scratching". Increasing the silica content leads to the same pits encountered with higher acid concentrations, and deletion produces an orange-peel effect across the crystal face.

On the "B" face, the same etchant produces an orange-peel texture and "scratches". An etchant consisting of 150ml HCl and 5g $AlCl_3$ per 1000 ml H_2O, on a Pellon Pan-W polishing pad produces somewhat better results. Shallow scratches were apparent when the surface was viewed by Nomarski microscopy at 400 x magnification although no

preferential etching or orange-peel effect was observable (see Figure 2).

Polished "A"-surfaces were also examined by low-energy electron diffraction (LEED) and Auger spectroscopy at 10^{-9} Torr using a hemispherical grid apparatus. A 1-minute flash to 450°C was sufficient to generate the sharp (1x1) LEED pattern shown in Figure 3, whereas ion bombardment is generally required to generate any LEED pattern on CdS(4) and other semiconductors. The diffraction pattern was observable down to 20 eV, below which surface charging became a problem, and up to 180 eV, above which the diffraction features faded into the diffuse background. Table I compares Auger spectra taken before and after the 450°C flash. C and Cl were the only contaminants detected. Both of these were reduced considerably, though not completely eliminated, by the 450°C flash, with accompanying increases in the Cd and S signals. Based on the quality of the LEED pattern and on relative Auger peak strengths, residual contamination is estimated to be about 1/10 monolayer.

ACKNOWLEDGEMENTS

The author expresses his appreciation to Robert McGraw for invaluable consultations. This research was supported by the Advanced Research Projects Agency of the Department of Defense and was monitored by ONR under Contract No. N00014-73-C-0280.

REFERENCES

1. M. V. Sullivan and W. R. Bracht, J. Electrochem. Soc. 114, 295 (1967)

2. W. H. Strehlow, J. Appl. Phys. 40, 2928 (1969)

3. E. P. Warekois, M. C. Lavine, A. N. Mariano, and H. C. Gatos, J. Appl. Phys. 33, 690 (1962)

4. L. R. Bedell and H. E. Farnsworth, Surf. Sci. 41, 165 (1974)

TABLE I

Auger Spectra of CdS(0001A)

element	nominal eV	Auger peak strengths, V	
		before flash	after flash
S	152	78	109
Cl	181	1.0	0.4
C	272	3.6	2.4
Cd	277,283		
Cd	321	2.1	2.7
Cd	376,382	16.6	19.2
O	510	<0.1	<0.1

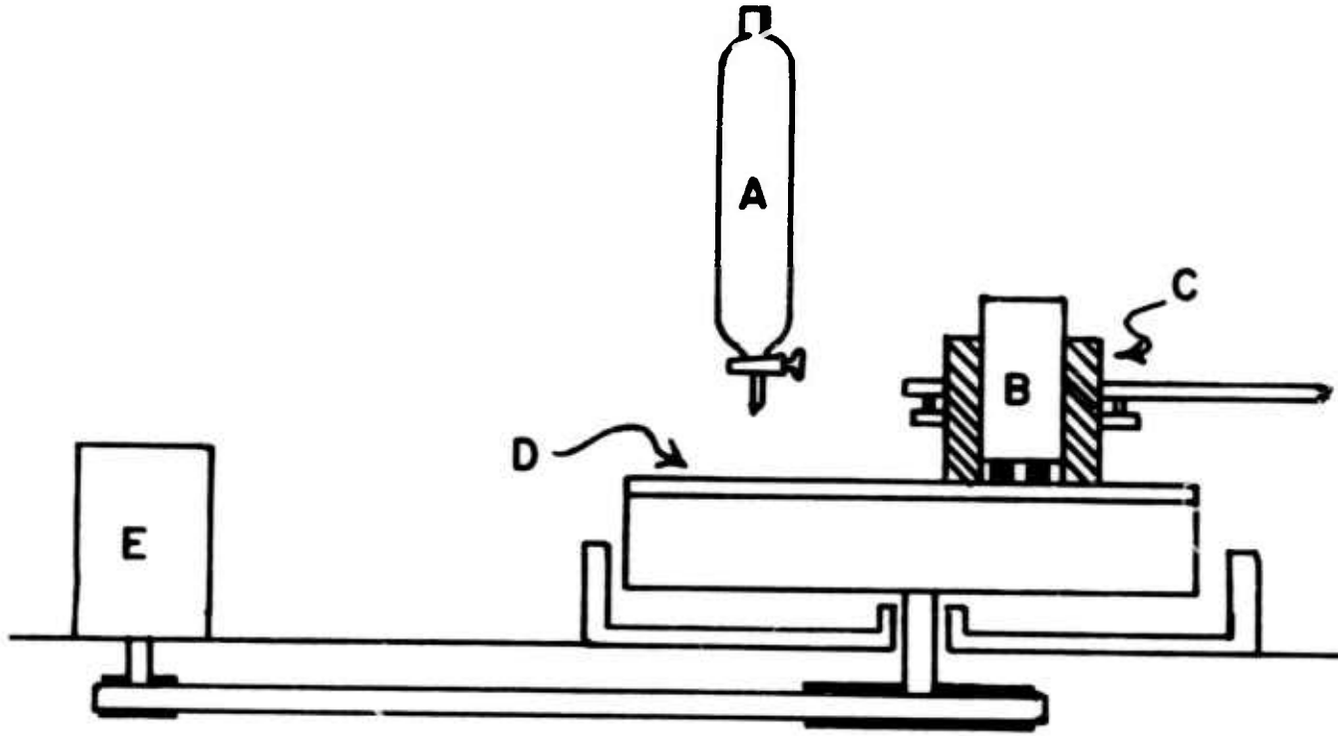

Figure 1: Schematic of chemomechanical polishing equipment: A, separating funnel; B, polishing block containing crystals; C, dressing ring; D, polishing pad; E, motor drive.

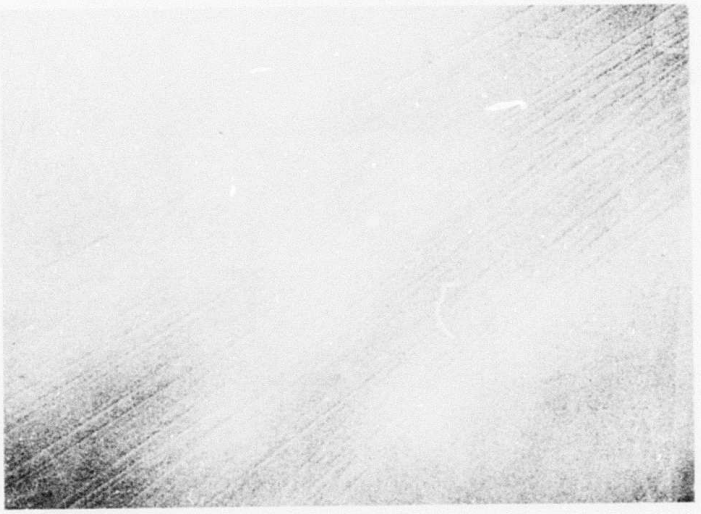

Figure 2: "B" face of polished CdS when viewed by Nomarski microscopy at 400 x magnification.

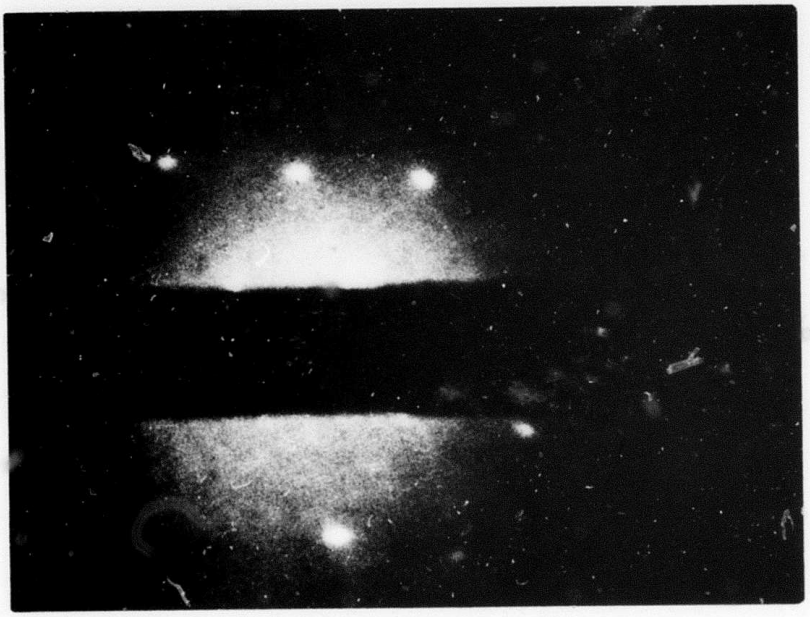

Figure 3: LEED pattern of polished CdS after 450° flash; 92 eV.